BIOCHEMISTRY
including biophysical chemistry & molecular biology

Article

pubs.acs.org/biochemistry

Residues Flanking Scissile Bonds in Factor VIII Modulate Rates of Cleavage and Proteolytic Activation Catalyzed by Factor Xa

Amy E. Griffiths, Jennifer Wintermute, Jennifer L. Newell-Caito,[†] and Philip J. Fay*

Department of Biochemistry and Biophysics, University of Rochester School of Medicine, 601 Elmwood Avenue, Rochester, New York 14642, United States

ABSTRACT: Factor Xa (FXa) proteolytically activates Factor VIII (FVIII) by cleaving P1 residues Arg^{372}, Arg^{740}, and Arg^{1689}. The Arg^{372} site represents the rate-limiting step for procofactor activation, whereas cleavage at Arg^{740} is a fast step. FXa also catalyzes inactivating cleavages that occur on a slower time scale than the activating ones. To assess the role of sequences flanking the Arg^{372} and Arg^{740} sites, recombinant FVIII variants in which P3−P3′ sequences were swapped individually or in combination were prepared. Replacing the Arg^{372} flanking sequence with that from the Arg^{740} site increased the rate of cleavage at Arg^{372}, as judged by the ∼5-fold increased rate in A1 subunit generation, and reduced the FVIIIa-dependent lag time for *in situ* FXa generation. The reciprocal swap yielded a nearly 2-fold increase in the rate of Arg^{372} cleavage, while the combined double-swap variant showed a 10-fold rate increase at that site, consistent with the individual effects being additive. Although this cleavage represents the slow step for activation, the rate of this reaction appeared to be ∼9-fold greater than the rate of the primary inactivating cleavage at Arg^{336} in generating the $A1^{336}$ product. Interestingly, replacement of the Arg^{372} flanking sequence with the Arg^{740} sequence combined with an Arg^{740}Gln mutation yielded both more rapid cleavage of the Arg^{372} site and accelerated inactivating cleavages within the A1 subunit. These results indicate that flanking sequences in part modulate the reaction rates required for procofactor activation and influence the capacity of FXa as an initial activator of FVIII rather than an inactivator.

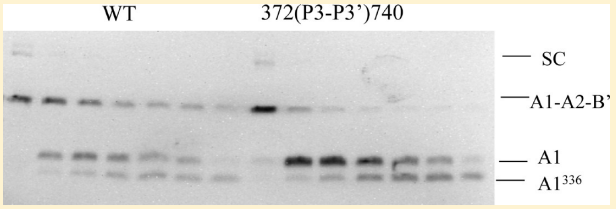

The blood coagulation procofactor factor VIII is synthesized as a single-chain, 2332-amino acid polypeptide.[1−3] The protein contains three domain types arranged as A1−a1−A2−a2−B−a3−A3−C1−C2, where short segments designated with the letter *a* are rich in acidic residues and the B domain is not essential for cofactor activity.[2,3] FVIII circulates in plasma as a heterodimer[4,5] comprised of a heavy chain consisting of the A1 and A2 domains and a light chain consisting of the A3, C1, and C2 domains.[3] The procofactor FVIII is converted to its active form, FVIIIa, by limited proteolysis by the serine protease thrombin or FXa following cleavages at P1 arginine residues[a] 372, 740, and 1689.[6] Cleavage at Arg^{372} is rate-limiting[7] and essential for the activation of FVIII in that this step exposes FIXa-interactive sites in FVIIIa that are otherwise masked in the procofactor.[8] FVIIIa associates with the serine protease FIXa on the phospholipid membrane to form the intrinsic FXase complex that activates FX during the propagation phase of coagulation (see ref 9 for a review).

While both thrombin and FXa activate FVIII, thrombin demonstrates a several-fold greater catalytic efficiency (k_{cat}/K_M) for FVIII[10] and thus may represent the dominant activator of the procofactor *in vivo*. In addition, thrombin activity toward FVIII is somewhat enhanced by the presence of von Willebrand factor (VWF),[11] whereas VWF blocks the FVIII−membrane interaction,[12] which is needed for efficient catalysis by FXa.[9] However, experiments have shown that porcine FVIIIa produced by FXa is more stable than thrombin-activated FVIIIa.[13] Furthermore, anionic phospholipid vesicles compete for FVIII binding with VWF,[12] indicating a distribution of FVIII between VWF and membranes at sites of vessel wall damage, and initial concentrations of FXa resulting from the initiation phase of clotting approach that of thrombin,[14] suggesting a potential contribution of FXa as a FVIII activator.

Downregulation of FXase results from inhibition of FVIIIa activity and occurs by mechanisms including subunit dissociation and proteolytic inactivation. The observed "self-dampening" of FXase results from A2 subunit dissociation, and this represents a physiologic mechanism for limiting FXa production.[9] The proteolytic pathway for FXase decay is mediated by activated protein C (APC)[15] and/or FXa.[16] Both proteinases cleave FVIIIa initially at Arg^{336},[6] preceding the acidic region (a1) of the A1 subunit and at a slower-reacting secondary site, Arg^{562},[17,18] bisecting the A2 subunit. An additional FXa cleavage site at Lys^{36} also correlates with FVIIIa inactivation.[19] Sequences flanking the Arg^{336} and Arg^{562} cleavage sites make significant contributions to rates of APC-catalyzed[20] and FXa-catalyzed[16] inactivation of FVIIIa, as judged by the capacity to modulate rates of cleavage by swapping these flanking sequences.

Previous studies of the coagulation proteases have shown that while exosite interactions play a major role in substrate affinity and specificity, the catalytic rate is controlled in large part by substrate docking at the active site.[21] We recently showed that changing the residues flanking selected scissile

Received: July 26, 2013
Revised: October 2, 2013
Published: October 15, 2013

bonds in FVIII can markedly alter the thrombin-catalyzed cleavage rates at these bonds, indicating a preference for certain cleavage-optimal residues.[22] Using a similar panel of variant FVIII proteins, we examine the effects of flanking sequences on the activating cleavages catalyzed by FXa. Results from this study indicate that via alteration of the residues surrounding the Arg^{372} and Arg^{740} cleavage sites, the rates of FXa-catalyzed cleavage and procofactor activation, as well as subsequent proteolytic inactivation, may be significantly altered.

EXPERIMENTAL PROCEDURES

Reagents. Monoclonal antibodies 58.12, which recognizes the N-terminus of the A1 domain of FVIII, and 2D2, which recognizes the N-terminus of the A3 domain, were gifts from Bayer Corp. (Berkeley, CA). The C5 antibody, which recognizes the C-terminal region of the A1 subunit, was a gift from Z. Ruggeri. The R8B12 antibody, recognizing the C-terminus of the A2 domain, was obtained from Green Mountain Antibodies (Burlington, VT). Phospholipid vesicles containing 20% phosphatidylserine, 40% phosphatidylcholine, and 40% phosphatidylethanolamine were prepared as described previously.[23] Coagulation proteins FIXa, FX, and FXa were obtained from Enzyme Research Laboratories (South Bend, IN), and Pefa-5523 chromogenic substrate was from Centerchem (Norwalk, CT).

Construction, Expression, and Purification of Recombinant Proteins. Recombinant FVIII variants used in this study were constructed as B-domainless FVIII forms, stably transfected into baby hamster kidney cells, and purified as described previously.[22] These FVIII variants include the flanking sequence swap mutations designated 372(P3−P3′)740, 740(P3−P3′)372, 372(P3−P3′)740/R740Q, and 372(P3−P3′)740/740(P3−P3′)372. For example, FVIII 372(P3−P3′)740 indicates a variant in which the P3−P3′ residues flanking Arg^{372} are replaced with those flanking Arg^{740}. Specific activity values were calculated from FVIII concentrations determined by an enzyme-linked immunosorbent assay[24] and activity determined by a one-stage clotting assay. The specific activity for 372(P3−P3′)740/R740Q was modestly reduced (38%) compared with that of WT [4.5 ± 0.6 units/μg (100% value)], while 372(P3−P3′)740, 740(P3−P3′)372, and 372(P3−P3′)740/740(P3−P3′)372 variants showed essentially normal phenotypes with specific activity values that were 68, 73, and 122%, respectively, of the WT value.[22]

FXa Cleavage of FVIII. WT or mutant FVIII (100 nM) was incubated in the presence of phospholipid vesicles (10 μM) at 22 °C with the indicated concentrations of FXa (see figure legends) in a buffer containing 20 mM HEPES (pH 7.2), 0.14 M NaCl, 5 mM $CaCl_2$, and 0.01% Tween 20. Samples were removed at the indicated time points, and reactions were terminated by addition to SDS−PAGE sample buffer [0.04 M Tris-HCl, 2% (w/v) SDS, 4% (v/v) glycerol, and 0.05% bromophenol blue (pH 6.8)] containing 3% (v/v) 2-mercaptoethanol and mixtures boiled for 5 min. Cleavage rates were assessed by rates of $A1^{336}$, A1, A2, and/or A3−C1−C2 subunit generation.

Electrophoresis and Western Blotting. FXa cleavage of WT and mutant FVIII was evaluated by SDS−PAGE[25] on 8% polyacrylamide gels using a Bio-Rad mini-gel apparatus at 175 V for 1 h. Protein transfer was performed using a polyvinylidene fluoride membrane for 1 h at 100 V in ice-cold transfer buffer [10 mM 3-(cyclohexylamino)propane-1-sulfonic acid and 10% (v/v) methanol (pH 11)]. Western blotting was performed by probing the membranes with anti-FVIII monoclonal antibodies 58.12, R8B12, and 2D2, for the A1, A2, and A3−C1−C2 subunits, respectively. The alkaline phosphatase-linked goat anti-mouse antibody (Sigma) was used as a secondary antibody for band detection. Blots were developed using the enhanced chemifluorescence (Amersham) system and scanned at 565 nm on a Bio-Rad VersaDoc Imaging System. Densitometry was used to quantitate the linear density regions of the blots using ImageLab (Bio-Rad).

Determination of Rates of Subunit Generation. All experiments were performed at least three times, and average values with standard deviations are shown. The intensity of each band was determined by volume integration and corrected for variability in background staining by using densities in the areas immediately adjacent to each band, with densitometry performed in regions of linear band density whenever possible. The concentrations of each subunit were normalized to the total density in each lane to correct for any differences in loading. Time points were fit using nonlinear least-squares regression to the single-exponential equation

$$A = A_o(1 - e^{-k_{obs}t})$$

where A_o is the total nanomolar concentration of the individual subunit and t is the time in minutes. The absolute value of k_{obs} represents the rate of subunit generation normalized by the FXa concentration and is expressed in nanomoles of subunit per minute per nanomole of FXa. The quality of the fitted data was acceptable, with R^2 values of >0.95.

FXa Generation Assay. The rates of FXa generation using WT and variant FVIII were monitored in a purified system.[26] Factor VIII (1 nM) in 20 μM phospholipid vesicles and 20 mM HEPES (pH 7.2), 100 mM NaCl, 5 mM $CaCl_2$, 0.01% Tween 20, and 100 μg/mL bovine serum albumin was incubated at 22 °C. Reactions were initiated by addition of FIXa and FX to final concentrations of 10 and 300 nM, respectively, and aliquots were removed at the indicated times, added to tubes containing EDTA (final concentration of 50 mM), and boiled for 5 min. Rates of FXa generation were determined by the addition of chromogenic substrate Pefa-5523 (final concentration of 0.46 mM) and read for 5 min at 385 nM using a V_{max} microtiter plate reader (Molecular Devices). Plotted data points are averages of three separate experiments. No FXa or thrombin was detected in the preparation of either FX or FIXa.

RESULTS

FXa-Catalyzed Cleavages of WT FVIII Leading to Procofactor Activation. FXa activates FVIII to FVIIIa following proteolytic cleavages similar to those identified for thrombin. The FVIII substrates employed in this study are expressed in nearly equal amounts of single-chain FVIII (Figure 1A) and FVIII heterodimer (Figure 1B). Both substrates are efficiently cleaved by FXa, resulting in the generation of A1, A2, and A3−C1−C2 FVIIIa subunits (Figure 2). Generation of the A1 subunit results from a single cleavage by FXa at Arg^{372}. Therefore, the rate of cleavage at that residue is equivalent to the rate of A1 subunit generation. The heavy chain of the heterodimeric form of FVIII requires only cleavage at Arg^{372} for generation of the A2 subunit in the heterodimer, but in the single-chain form, cleavages at both Arg^{372} and Arg^{740} are required. Because the presence or absence of the 14-residue B domain remnant following the A2 domain cannot be discerned

dx.doi.org/10.1021/bi4010123 | Biochemistry 2013, 52, 8060−8068

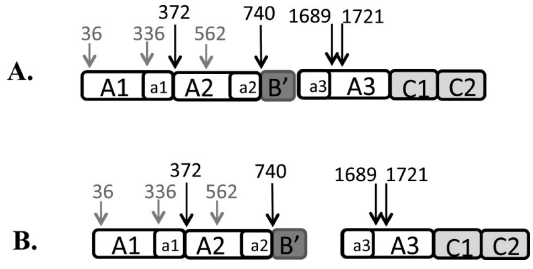

Figure 1. Forms of B-domainless FVIII secreted from BHK cells. Schematics of single-chain (A) and heterodimeric (B) forms of FVIII show the domain organization, where B′ represents a 14-residue segment of the original B domain. FXa cleavage sites are marked by arrows, with labels of activating cleavages of FVIII colored black and labels of inactivating cleavages of FVIIIa colored gray.

using SDS−PAGE, it is not possible to directly determine the rate of cleavage at Arg^{740} in recombinant B-domainless FVIII. However, rates of A2 subunit generation are used in this study to compare the WT value to variant values. A single cleavage at Arg^{1689} in both the light chain and single chain yields the A3−C1−C2 subunit. Therefore, the rate of generation of this subunit represents the rate of Arg^{1689} cleavage. Factor Xa is also known to cleave FVIII at Arg^{1721},[6] and the detection of protein cleaved at Arg^{1689} and Arg^{1721} could be attributed to the lack of clarity of these bands in the Western blots. We note that the 2D2 epitope has recently been mapped to A3 domain residues 1801−1805;[27] thus, cleavage at either Arg^{1689} or Arg^{1721} is detected as a large product. Furthermore, two additional sites for FXa cleavage are noted, Lys^{36} and Arg^{336}. Cleavage at these sites results in the inactivation of FVIII. While the latter site is cleaved at approximately twice the rate of the former, cleavage at either site is much slower (<10-fold) than that of the activating cleavage at Arg^{372}.[28] These slow rates coupled with an inherent imprecision in the blotting technique justify use of the single-site exponential equation to estimate the rates of A1 subunit generation.

Reaction of WT FVIII with FXa was conducted over a 25 min time course and visualized using SDS−PAGE and Western blotting as described in Experimental Procedures. WT FVIII controls were run under identical conditions with each of the FVIII variants (Figures 2 and 3). Data quantitating the blots in Figure 4 showed that the rates of generation of the A1, A2, and A3−C1−C2 products increased over time, with maximal levels

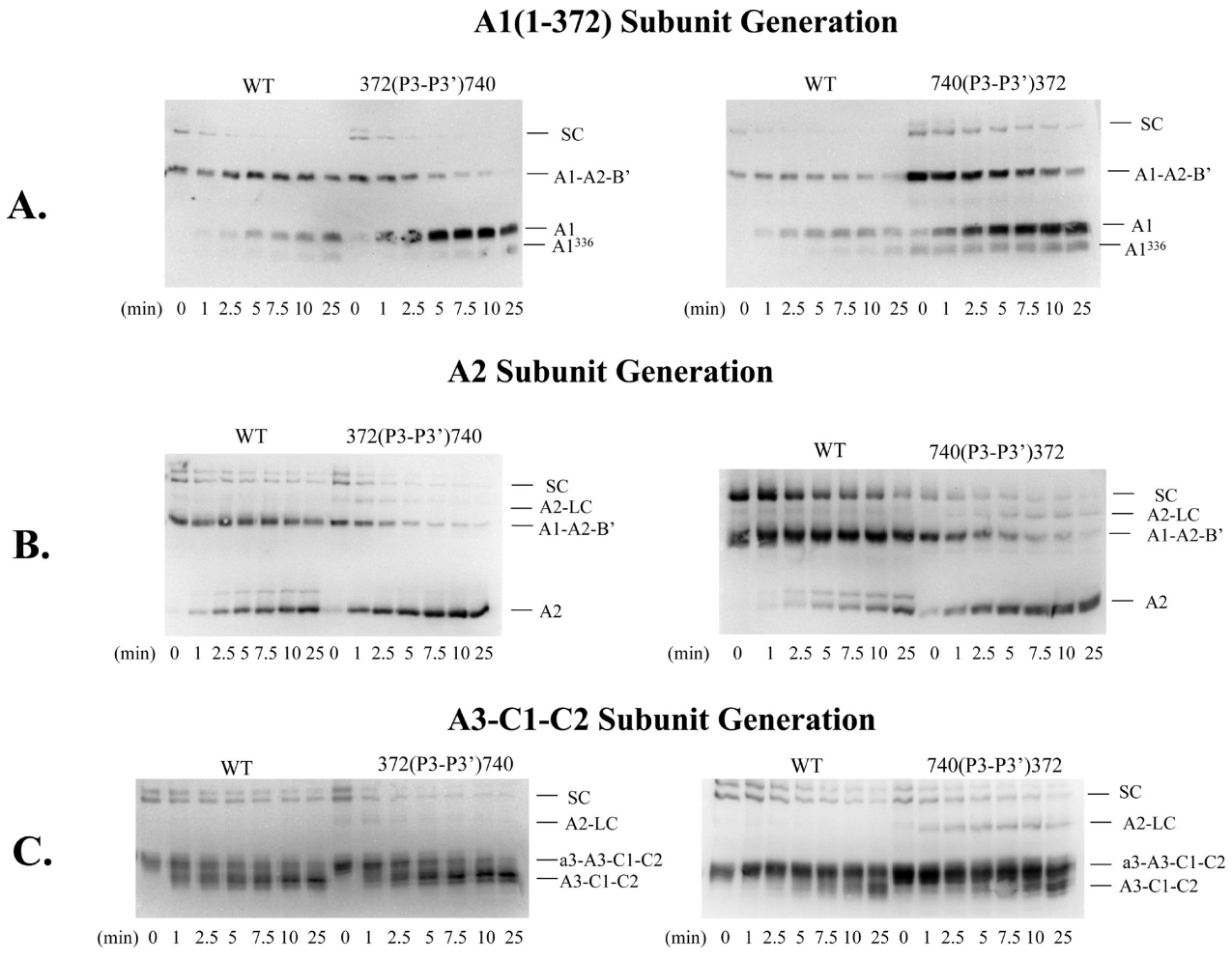

Figure 2. FXa cleavage of the single-swap P3−P3′ FVIII mutants. The WT and 372(P3−P3′)740 and 740(P3−P3′)372 FVIII variants (100 nM) were reacted with FXa over a 25 min time course, and samples were subjected to Western blotting for detection of A1, A2, and A3−C1−C2 subunits as described in Experimental Procedures. Shown are representative blots for rates of (A) A1 subunit generation for reactions using 2 nM FXa, (B) A2 subunit generation using 2 nM FXa, and (C) A3−C1−C2 subunit generation using 10 nM FXa for the left blot and 1 nM for the right blot. SC and LC refer to single chain and light chain, respectively.

dx.doi.org/10.1021/bi4010123 | *Biochemistry* 2013, 52, 8060−8068

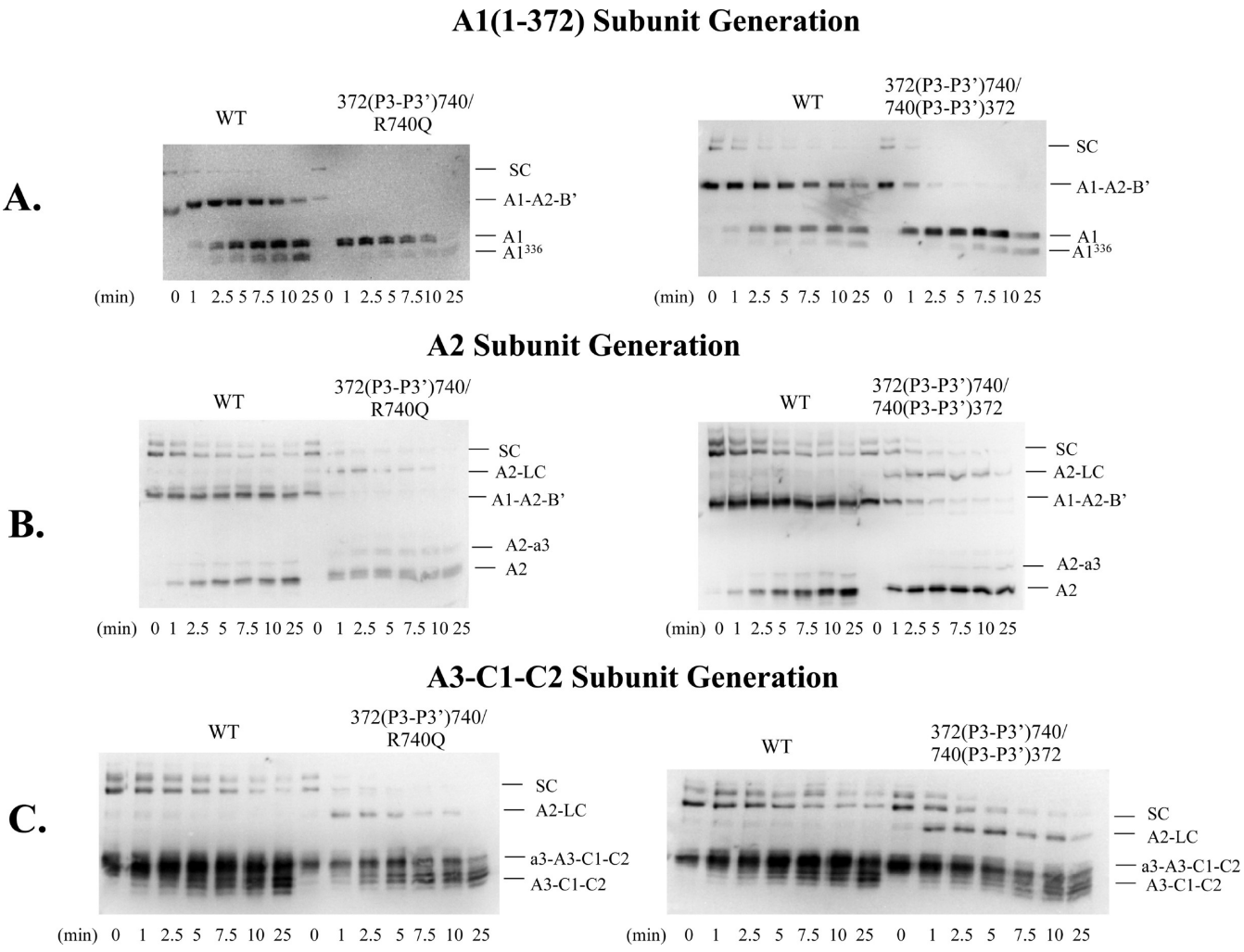

Figure 3. FXa cleavage of the combination P3−P3′ FVIII mutants. The WT and 372(P3−P3′)740/R740Q and 372(P3−P3′)740/740(P3−P3′)372 FVIII variants (100 nM) were reacted with FXa over a 25 min time course, and samples were subjected to Western blotting for detection of A1, A2, and A3−C1−C2 subunits as described in Experimental Procedures. Shown are representative blots for rates of (A) A1 subunit generation for reactions using 2 nM FXa, (B) A2 subunit generation using 2 nM FXa for the left blot and 1 nM FXa for the right blot, and (C) A3−C1−C2 subunit generation using 2 nM FXa for the left blot and 1 nM for the right blot. SC and LC refer to single chain and light chain, respectively.

reached at approximately 10 min. Cleavage rate values extracted from these curves for WT FVIII showed similar rates for A1 and A2 subunit generation, while the rate for A3−C1−C2 subunit generation was possibly somewhat faster (Table 1). The A1 subunit is further cleaved at Arg^{336} and Lys^{36}. These results are consistent with the Arg^{372} site representing the slow step in the activation process because generation of A2 from the single chain also requires cleavage at Arg^{740}. We also note that cleavage of WT FVIII yielding the $A1^{336}$ product correlating with FVIII inactivation occurs at a rate ∼9-fold slower than that of the rate-limiting cleavage separating the A1 and A2 domains during procofactor activation. Thus, most of the FVIII procofactor has been converted to cofactor prior to this event. Because the A1 subunit is slowly cleaved at Arg^{336} and Lys^{36},[28] the rate value presented for A1 subunit generation represents an estimated value.

Factor Xa-Catalyzed Cleavage of Single-Swap Recombinant FVIII Mutants. Replacing the sequences flanking Arg^{372} with those from Arg^{740} in the 372(P3−P3′)740 variant resulted in a marked acceleration (∼4−5-fold) of cleavage at Arg^{372} relative to that of WT as judged by the acceleration of the appearance of A1 and A2 subunits (Figures 2 and 4 and Table 1). These results indicate that the flanking sequences surrounding the Arg^{740} site are more optimal for cleavage by FXa. Furthermore, this swap did not appreciably influence the rate of cleavage in the FVIII light chain, suggesting that reactions at the heavy chain and light chain sites by FXa are independent rather than linked cleavage events. On the other hand, when we replaced the fast-reacting Arg^{740} flanking sequence with the slow-reacting one surrounding Arg^{372}, we noted an ∼3-fold decrease in the rate of cleavage of the A1 subunit compared with that seen with the reciprocal swap. However, this value was still marginally (<2-fold) greater than the rate observed for WT FVIII. Similar results were observed for the generation of the A2 subunit, while again, no effect on rate of the generation of the A3−C1−C2 subunit resulted from this swap in the heavy chain sequences. These results suggest that altering the cleavage rate at Arg^{740} impacts the rate of cleavage at Arg^{372}, supporting a linkage of these cleavage events.

Factor Xa-Catalyzed Cleavage of Combination Recombinant FVIII Mutants. Two additional FVIII variants that contained the 372(P3−P3′)740 swap plus an additional mutation were evaluated. In one variant, the Arg^{740} residue was replaced with a noncleavable Gln residue to yield the

dx.doi.org/10.1021/bi4010123 | Biochemistry 2013, 52, 8060−8068

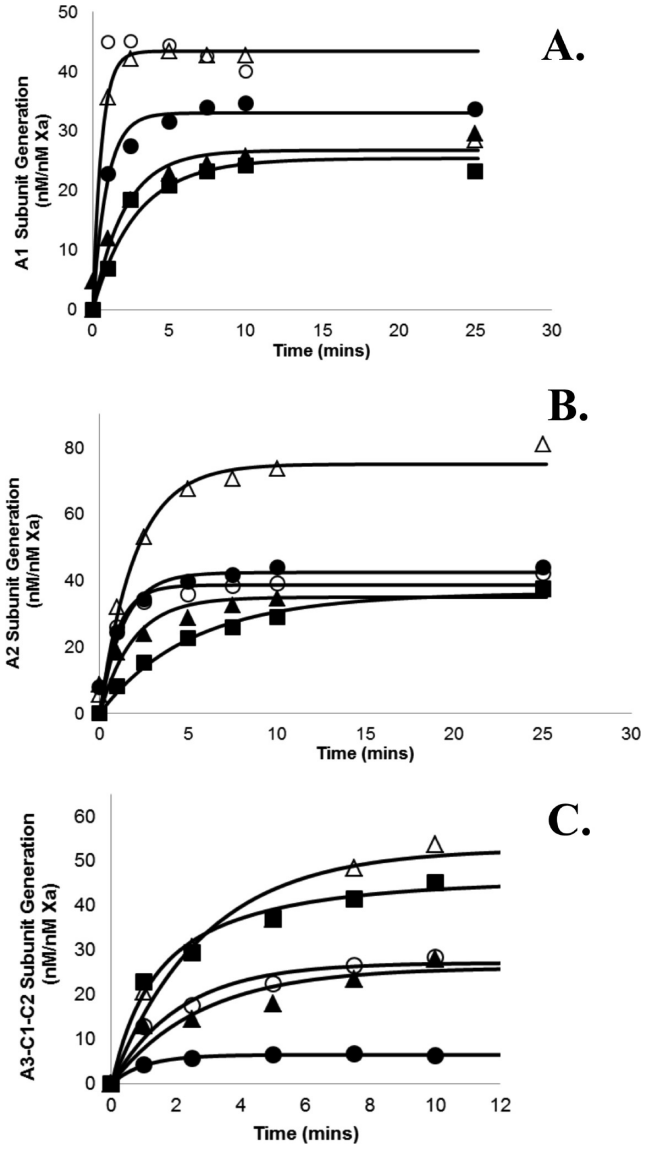

Figure 4. Analysis of the Western blots of the FVIII mutants. Rates derived from the densitometry scans for the Western blots shown in Figures 2 and 3 are shown. Rates of generation are shown for A1 (A), A2 (B), and A3−C1−C2 (C) subunits, for FVIII WT (■), 372(P3−P3′)740 (●), 372(P3−P3′)740/R740Q (○), 740(P3−P3′)372 (▲), and 372(P3−P3′)740/740(P3−P3′)372 (△). Lines are drawn representing the time points fit to the single-exponential equation using nonlinear least-squares regression as described in Experimental Procedures. Experiments were performed at least three individual times, and average values are shown.

variant designated 372(P3−P3′)740/R740Q. In a second variant, a reciprocal swap was made to include 372(P3−P3′)740 with 740(P3−P3′)372. Thus, in the former variant, we would predict cleavage at the A1−A2 junction would be enhanced while cleavage at the A2−B junction abrogated, whereas in the latter variant, we may predict accelerated cleavage at the A1−A2 junction with a rate reduction at the A2−B junction. Results from Western blotting are shown in Figure 3. The time course of cleavage using the 372(P3−P3′)740/R740Q variant (Figure 3A, left panel) yielded an unusual pattern of cleavage for the heavy chain-derived products. A1 subunit generation occurred very quickly with essentially all substrate converted to A1 within 1 min. Furthermore, all bands reactive with the anti-A1 domain antibody (58.12) disappeared 5−7 min into the time course. For these reasons, a rate value was not determined. We speculate this fast cleavage rate results from failure of the FXa active site to engage the Gln at position 740 but rather rapidly engages the Arg^{372} now flanked by more cleavage-optimal residues from residue 740. We also suggest that the loss of antibody-reactive bands results from accelerated cleavage at Lys^{36}, a minor inactivating cleavage site,[19] inasmuch as this cleavage removes the epitope for antibody 58.12 (residues 6−15[27]). Blots with C-terminal A1 antibody C5 (not shown) show replacement of virtually all intact A1 (residues 1−372) by truncated A1 (residues 336−372) by the 10 min point. Blots with this variant using the anti-A2 antibody were consistently faint. One reason for this is that two A2 subunit products were obtained (Figure 3B, left panel), the authentic A2 subunit derived from the FVIII heterodimer and an A2−a3 subunit derived from single-chain FVIII. This latter product results from cleavage at Arg^{1689} after the cleavage site at Arg^{740} has been eliminated. Thus, this product, which migrates more slowly than the authentic A2 subunit in the gel, contains the A2 domain, the 14-residue B domain remnant, and the a3 acidic region (see Figure 1).

The FVIII 372(P3−P3′)740/740(P3−P3′)372 variant combining both the flanking sequence swaps showed a significantly increased rate of cleavage at Arg^{372} (Figure 3A, right panel) that was 10-fold greater than the rate determined for WT FVIII (Table 1). This result likely reflected a synergy of the enhanced rates observed for the 372(P3−P3′)740 component swap (5-fold) and the 740(P3−P3′)372 component swap (∼2-fold). The rate of A2 subunit generation may be slightly increased versus the rate observed for the 372(P3−P3′)740 variant. In addition, we observed a modest increase (<2-fold) versus the value of the WT at the a3−A3 junction, leading to generation of the A3−C1−C2 subunit.

Table 1. Rates of A1, A2, and A3−C1−C2 Subunit Generation during WT and P3−P3′ Mutant Activation by FXa[a]

	$A1^{336}$ subunit generation [nmol of $A1^{336}$ min^{-1} (nmol of FXa)$^{-1}$]	A1 subunit generation [nmol of A1 min^{-1} (nmol of FXa)$^{-1}$]	A2 subunit generation [nmol of A2 min^{-1} (nmol of FXa)$^{-1}$]	A3−C1−C2 subunit generation [nmol of A3−C1−C2 min^{-1} (nmol of FXa)$^{-1}$]
WT	0.87 ± 0.19	7.6 ± 0.53	7.1 ± 0.9	10.3 ± 3.0
372(P3−P3′)740	0.76 ± 0.0076	34.5 ± 3.6	32.2 ± 4.5	6.42 ± 1.2
740(P3−P3′)372	1.18 ± 0.10	12.7 ± 0.21	46.3 ± 7.4	9.3 ± 0.2
372(P3−P3′)740/R740Q	3.70 ± 0.40	could not be determined	39.4 ± 1.2	12.7 ± 1.1
372(P3−P3′)740/740(P3−P3′)372	1.14 ± 0.13	75.5 ± 13.7	37.9 ± 1.3	18.1 ± 0.6

[a]Rates of $A1^{336}$, A1, A2, and A3−C1−C2 subunit generation by FXa cleavage of WT and FVIIIa were estimated by nonlinear least-squares regression analysis of the data shown in Figures 2−4, 6, and 7. The data represent averages ± the standard deviation of at least three experiments. Western blot assays were performed and data analyzed as described in Experimental Procedures.

dx.doi.org/10.1021/bi4010123 | *Biochemistry* 2013, 52, 8060−8068

Factor Xa Generation Assay. Results from the proteolysis data were compared with the capacity for FXa to activate FVIII. Because FXa is the product of the FXa generation assay used to monitor FVIIIa function, we omitted the addition of exogenous FXa from the reaction. Instead, FVIII was added to a reaction mixture containing FIXa and phospholipid vesicles, and reactions were initiated with FX as described in Experimental Procedures. Using this design, a lag period is observed until low levels of FXa are generated in a FVIII-independent manner. However, once generated, FXa activates FVIII, and the reaction proceeds at a markedly increased rate. Thus, the lag time preceding this activity burst correlates with the time for FVIII activation.

Results from this analysis for the WT and variants are shown in Figure 5. FVIII WT exhibited a lag of ~2 min. Three of the four mutants tested showed a decrease in their initial lag time in comparison to that of the WT. For the first three minutes, the 372(P3−P3′)740/740(P3−P3′)372 and 740(P3−P3′)372 variants showed enhanced FXa production compared with that of the WT, with 372(P3−P3′)740 showing the most dramatic increase in the rate of FXa generation after the initial lag. This variant produced FXa more efficiently than the WT past a time of 6 min, or past 10 min at lower FVIII concentrations. The one mutant that showed rates slower than that of the WT over the time course was 372(P3−P3′)740/R740Q, which is consistent with the results that show FXa is contributing to inactivating cleavage of this variant at Lys^{36} and/or Arg^{336}.

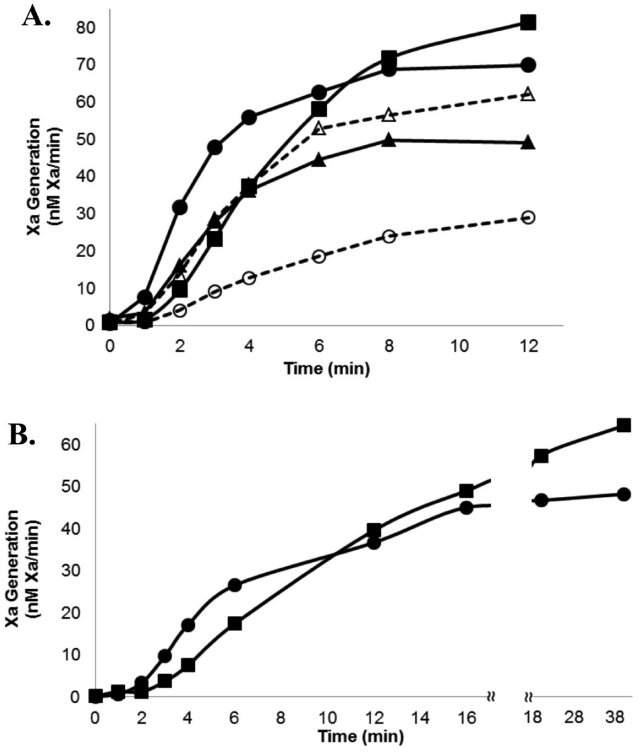

Figure 5. Factor Xa-generating activity of the FVIII mutants. Factor Xa generation assays were run as described in Experimental Procedures, using 20 μM phospholipid vesicles, 10 nM FIXa, 300 nM FX, and 0.3 nM (A) and 0.1 nM (B) WT or variant FVIII. Rates of generation are shown for WT FVIII (■, solid line), 372(P3−P3′)740 (●, solid line), 372(P3−P3′)740/R740Q (○, dashed line), 740(P3−P3′)372 (▲, solid line), and 372(P3−P3′)740/740(P3−P3′)372 (△, dashed line). Experiments were performed at least three individual times, and average values are shown.

Factor Xa-Catalyzed Inactivation of Recombinant FVIII Mutants. In addition to its activating cleavages of FVIII, FXa inactivates FVIIIa by catalyzing cleavage at Arg^{336} and to a lesser extent at Lys^{36}. To determine whether the mutations surrounding the activating cleavage sites affected the FXa-catalyzed inactivation of FVIII, experiments were performed using 5−10-fold higher concentrations of FXa. The rate of cleavage at the primary inactivation site, Arg^{336}, which yields the truncated A1 subunit, A1^{336} (residues 1−336), was found to be ~9 times slower than the activating cleavage nearby at Arg^{372} for the WT protein (Figures 6 and 7). The rates of A1^{336} generation were similar to that of the WT for the three variants, 372(P3−P3′)740, 740(P3−P3′)372, and 372(P3−P3′)740/740(P3−P3′)372 (see Table 1). In contrast, 372(P3−P3′)740/R740Q showed a rate that appeared to be ~4-fold greater than those of the WT or the other mutants. However, as in assessing the rate of cleavage at the A1 site for this variant, we found quantitation of this value was difficult because of the loss of the anti-A1 epitope resulting from an apparent increase in the rate of cleavage at Lys^{36}. Thus, it appears that blocking the Arg^{740} site in FVIII combined with accelerating activation at Arg^{372} in turn accelerates the inactivation of FVIIIa by attack at both Arg^{336} and Lys^{36}.

DISCUSSION

Results presented in this report show that rates of FXa-catalyzed activation of FVIII can be markedly influenced by the sequences flanking the scissile bonds. Similar to thrombin-catalyzed activation, the rate-limiting step in this process is cleavage at Arg^{372} to separate the contiguous A1−A2 domains into individual subunits. We observed this rate could be accelerated ~5-fold as measured by the rate of A1 subunit generation, by replacing the P3−P3′ residues flanking Arg^{372} with those that flank the fast-reacting Arg^{740} cleavage site. Furthermore, a reciprocal swap to slow cleavage at Arg^{740} resulted in a modest acceleration (~2-fold) in the rate of cleavage at Arg^{372}, while the combined double swap yielded a 10-fold increase in rate versus that of the WT. These latter observations suggest that slowing the rate of FXa attack at Arg^{740} actually enhances the active site engagement of FXa at the Arg^{372} site. This conclusion was supported by results obtained when the 372(P3−P3′)740 swap was combined with an Arg^{740}Gln mutation to block active site engagement at the Arg^{740} site. Although the rate of cleavage of Arg^{372} could not be accurately determined for this variant because of apparent accelerated cofactor inactivation (see below), comparison of the blots shows a significantly more rapid rate of conversion of FVIII heavy chain to A1 subunit when the Arg^{740} residue cannot be cleaved.

In an earlier study,[22] these FVIII substrates were used to assess the role of flanking sequences in the mechanism for thrombin activation of the procofactor. In that report, replacing the P3−P3′ residues flanking Arg^{372} with those that flank the Arg^{740} cleavage site yielded a 10-fold increase in the rate of Arg^{372} cleavage, while the reciprocal swap resulted in a 2−3-fold rate increase. Interestingly, the combined swap did not yield a rate that was increased compared with that of the 372(P3−P3′)740 single-swap variant. Furthermore, similar to results in this study, rates of thrombin cleavage in the FVIII heavy chain domains did not appreciably affect the rate of light chain cleavage at the a3−A3 junction. Thus, activation of FVIII by

dx.doi.org/10.1021/bi4010123 | Biochemistry 2013, 52, 8060−8068

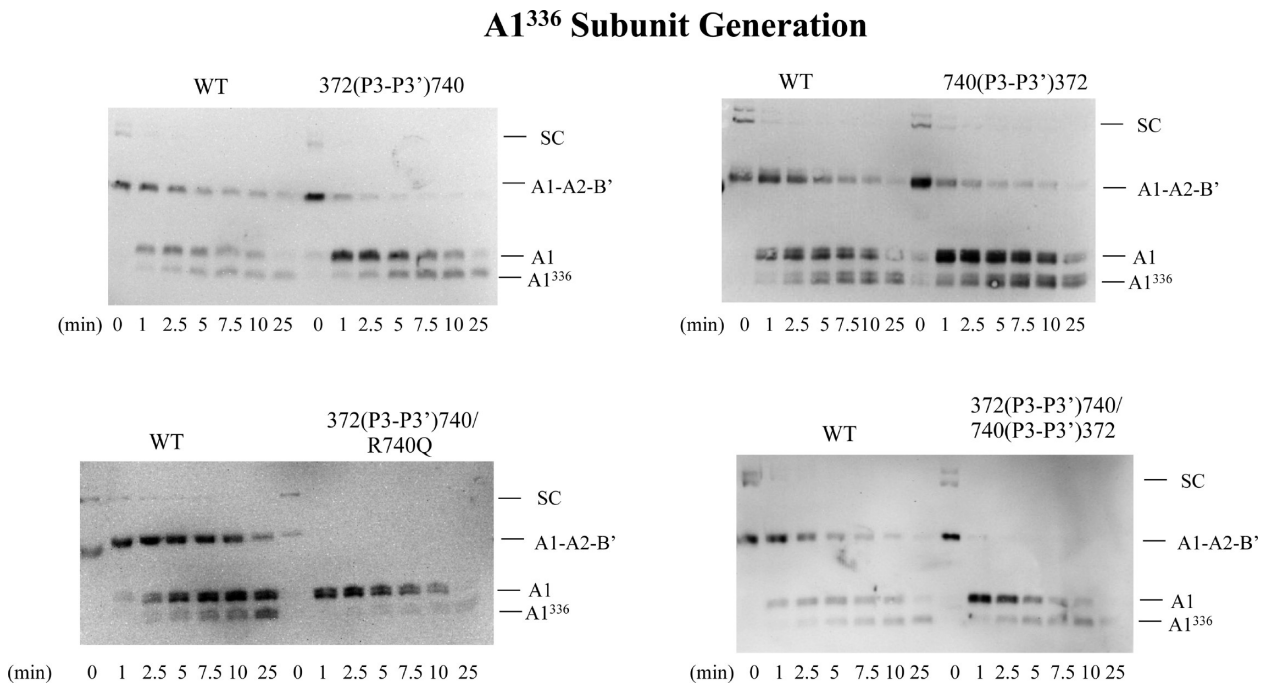

Figure 6. FXa cleavage of the P3−P3′ FVIII mutants. The WT and FVIII variants (100 nM) were reacted with FXa over a 25 min time course, and samples were subjected to Western blotting using monoclonal antibody 58.12 for detection of the A1 subunits as described in Experimental Procedures. Shown are representative blots, using 10 nM FXa for WT and variants in the blot for 372(P3−P3′)740, 740(P3−P3′)372, and 372(P3−P3′)740/740(P3−P3′)372, and 2 nM FXa for the 372(P3−P3′)740/R740Q blot. SC refers to single chain.

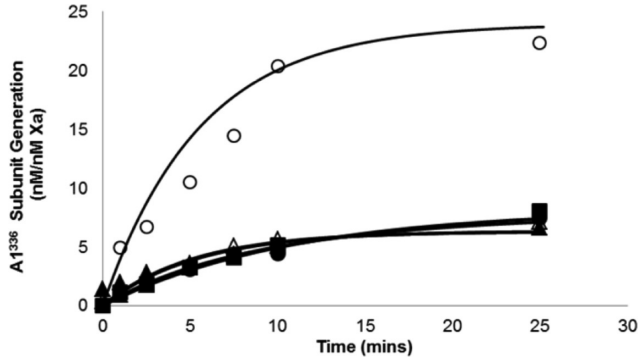

Figure 7. Analysis of the Western blots of the FVIII mutants. Rates of generation are shown for the $A1^{336}$ subunit for FVIII WT (■), 372(P3−P3′)740 (●), 372(P3−P3′)740/R740Q (○), 740(P3−P3′)372 (▲), and 372(P3−P3′)740/740(P3−P3′)372 (△), derived from the densitometry scans for the Western blots shown in Figure 5. Lines are drawn representing the time points fit to the single-exponential equation using nonlinear least-squares regression as described in Experimental Procedures. Experiments were performed at least three individual times, and average values are shown.

either enzyme is facilitated by sequences flanking the scissile bonds.

Unlike thrombin, FXa inactivates FVIII and FVIIIa primarily following cleavage at Arg^{336} [6] at the C-terminal region of the A1 subunit as well as at minor, slower-reacting sites within the A1 domain at Lys^{36} [19] and within the A2 domain at Arg^{562}.[18] We observed that the rate of cleavage of a WT FVIII substrate at the Arg^{336} site was ∼10% of that for the rate-limiting cleavage at Arg^{372}, consistent with procofactor activation as the primary pathway for reaction of FVIII with FXa. Altering sequences flanking the activation sites showed little if any effect on rates of cleavage at the Arg^{336} site. However, we did note that blocking cleavage at Arg^{740} with an Arg^{740}Gln mutation not only accelerated cleavage at the Arg^{372} site but also resulted in a loss of antibody reactivity at later time points. This observation was consistent with accelerated inactivation following cleavage at Lys^{36}, thereby removing the epitope for the 58.12 antibody used for detection, and also with the low activity of this variant based on the rate of FXa generated compared with the other variants.

In a recent study, DeAngelis et al.[16] examined the FXa-catalyzed inactivation of FVIIIa following replacement of sequences flanking Arg^{336} with those from the activation sites at Arg^{740} and Arg^{372}. Results from that study showed that both swaps accelerated the rate of cleavage at Arg^{336}, leading to increased rates of cofactor inactivation and reduced thrombin generation parameters in a hemophilia A-deficient plasma. Rates of cleavage at Arg^{336} were increased ∼6-fold for the swap flanking the Arg^{740} sequence and ∼2-fold for the swap using the Arg^{372} flanking sequence. Thus, rates for both FXa-catalyzed activation and inactivation are modulated in part by flanking sequences.

On the basis of determination of catalytic efficiencies (k_{cat}/K_M) for a library of small molecule substrates for FXa, Bianchini et al.[29] noted that the P2 and P1′ positions yield the greatest selectivity for FXa. Both Arg^{372} and Arg^{740} are followed by Ser, which is optimal at the P1′ position. Met follows Arg^{336}, and this substrate showed a >10-fold reduced catalytic efficiency compared with that of the Ser-containing substrate. This difference in the P1′ residue likely contributes in part to the preference for FXa for activating rather than inactivating FVIII. Furthermore, the observed faster cleavage at Arg^{740} compared with that at Arg^{372} during procofactor activation may reflect in part the P2 Pro^{739} compared with Ile^{371}, where Pro showed an ∼6-fold increased catalytic efficiency compared with that of Ile at the P2 position in the small molecule substrate.[29] This

dx.doi.org/10.1021/bi4010123 | Biochemistry 2013, 52, 8060−8068

preference for Pro at the P2 position was consistent with the enhanced rates of cleavage, as well as reduced lag times in the *in situ* FXa activity generation assay, we observed for the sequence swaps used in this study.

Overall, results from this study demonstrate a dependence on sequences flanking scissile bonds for efficient activation of FVIII by FXa. Furthermore, these results taken together with those from our recent study examining the role of flanking sequences in FXa-catalyzed inactivation of FVIIIa[16] indicate that these sequences both contribute to the order of bond cleavage during the activation process and dictate that initial reaction of FVIII with FXa results in proteolytic activation subsequent to proteolytic inactivation.

AUTHOR INFORMATION

Corresponding Author

*Department of Biochemistry and Biophysics, University of Rochester School of Medicine, 601 Elmwood Ave., Rochester, NY 14642. E-mail: philip_fay@urmc.rochester.edu. Phone: (585) 275-6576.

Present Address

[†]J.L.N.-C.: Department of Chemistry and Biochemistry, University of the Sciences, Philadelphia, PA 19104.

Funding

This work was supported by National Institutes of Health Grant HL38199.

Notes

The authors declare no competing financial interest.

ACKNOWLEDGMENTS

We thank Pete Lollar and John Healey for the gift of the FVIII cloning and expression vectors and Zaverio Ruggeri, Bill Church, and Lisa Regan for the C5, GMA-8003, and 58.12 and 2D2 monoclonal antibodies, respectively.

ABBREVIATIONS

BHK, baby hamster kidney; SDS−PAGE, sodium dodecyl sulfate−polyacrylamide gel electrophoresis; ELISA, enzyme-linked immunosorbent assay; WT, wild-type; FVIII, factor VIII; FVIIIa, factor VIIIa; FIXa, factor IXa; FX, factor X; FXa, factor Xa; APC, activated protein C; VWF, von Willebrand factor.

ADDITIONAL NOTE

[a]Residues flanking the scissile bond are denoted using the nomenclature of Schechter and Berger. Residues preceding the scissile bond are designated P1−P*n* extending toward the NH_2 terminus, and residues following the scissile bond are designated P1′−P*n*′ extending toward the COOH terminus.

REFERENCES

(1) Toole, J. J., Knopf, J. L., Wozney, J. M., Sultzman, L. A., Buecker, J. L., Pittman, D. D., Kaufman, R. J., Brown, E., Shoemaker, C., Orr, E. C., Amphlett, G. W., Foster, W. B., Coe, M. L., Knutson, G. J., Fass, D. N., and Hewick, R. M. (1984) Molecular cloning of a cDNA encoding human antihaemophilic factor. *Nature 312*, 342−347.

(2) Wood, W. I., Capon, D. J., Simonsen, C. C., Eaton, D. L., Gitschier, J., Keyt, B., Seeburg, P. H., Smith, D. H., Hollingshead, P., Wion, K. L., Delwart, E., Tuddenham, E. D. G., Vehar, G. A., and Lawn, R. M. (1984) Expression of active human factor VIII from recombinant DNA clones. *Nature 312*, 330−337.

(3) Vehar, G. A., Keyt, B., Eaton, D., Rodriguez, H., O'Brien, D. P., Rotblat, F., Oppermann, H., Keck, R., Wood, W. I., Harkins, R. N., Tuddenham, E. G. D., Lawn, R. M., and Capon, D. J. (1984) Structure of human factor VIII. *Nature 312*, 337−342.

(4) Fass, D. N., Knutson, G. J., and Katzmann, J. A. (1982) Monoclonal antibodies to porcine factor VIII coagulant and their use in the isolation of active coagulant protein. *Blood 59*, 594−600.

(5) Fay, P. J., Anderson, M. T., Chavin, S. I., and Marder, V. J. (1986) The size of human factor VIII heterodimers and the effects produced by thrombin. *Biochim. Biophys. Acta 871*, 268−278.

(6) Eaton, D. L., and Vehar, G. A. (1986) Factor VIII structure and proteolytic processing. *Prog. Hemostasis Thromb. 8*, 47−70.

(7) Newell, J. L., and Fay, P. J. (2007) Proteolysis at Arg740 facilitates subsequent bond cleavages during thrombin-catalyzed activation of factor VIII. *J. Biol. Chem. 282*, 25367−25375.

(8) Fay, P. J., Mastri, M., Koszelak, M. E., and Wakabayashi, H. (2001) Cleavage of factor VIII heavy chain is required for the functional interaction of A2 subunit with factor IXa. *J. Biol. Chem. 276*, 12434−12439.

(9) Fay, P. J. (2004) Activation of factor VIII and mechanisms of cofactor action. *Blood Rev. 18*, 1−15.

(10) Lollar, P., Knutson, G. J., and Fass, D. N. (1985) Activation of porcine factor VIII:C by thrombin and factor Xa. *Biochemistry 24*, 8056−8064.

(11) Hill-Eubanks, D. C., and Lollar, P. (1990) von Willebrand factor is a cofactor for thrombin-catalyzed cleavage of the factor VIII light chain. *J. Biol. Chem. 265*, 17854−17858.

(12) Saenko, E. L., and Scandella, D. (1995) A mechanism for inhibition of factor VIII binding to phospholipid by von Willebrand factor. *J. Biol. Chem. 270*, 13826−13833.

(13) Parker, E. T., Pohl, J., Blackburn, M. N., and Lollar, P. (1997) Subunit structure and function of porcine factor Xa-activated factor VIII. *Biochemistry 36*, 9365−9373.

(14) Hockin, M. F., Jones, K. C., Everse, S. J., and Mann, K. G. (2002) A model for the stoichiometric regulation of blood coagulation. *J. Biol. Chem. 277*, 18322−18333.

(15) Walker, F. J., and Fay, P. J. (1992) Regulation of blood coagulation by the protein C system. *FASEB J. 6*, 2561−2567.

(16) DeAngelis, J., Wakabayashi, H., and Fay, P. J. (2012) Sequences flanking Arg336 in factor VIIIa modulate factor Xa-catalyzed cleavage rates at this site and cofactor function. *J. Biol. Chem. 287*, 15409−15417.

(17) Fay, P. J., Smudzin, T. M., and Walker, F. J. (1991) Activated protein C-catalyzed inactivation of human factor VIII and factor VIIIa. Identification of cleavage sites and correlation of proteolysis with cofactor activity. *J. Biol. Chem. 266*, 20139−20145.

(18) Plantier, J. L., Rolli, V., Ducasse, C., Dargaud, Y., Enroljas, N., Bourerche, H., and Negrier, C. (2009) Activated factor X cleaves factor VIII at arginine 562, limiting its cofactor efficiency. *J. Thromb. Haemostasis 8*, 286−293.

(19) Nogami, K., Wakabayashi, H., Schmidt, K., and Fay, P. J. (2003) Altered interactions between the A1 and A2 subunits of factor VIIIa following cleavage of A1 subunit by factor Xa. *J. Biol. Chem. 278*, 1634−1641.

(20) Varfaj, F., Wakabayashi, H., and Fay, P. J. (2007) Residues surrounding Arg336 and Arg562 contribute to the disparate rates of proteolysis of factor VIIIa catalyzed by activated protein C. *J. Biol. Chem. 282*, 20264−20272.

(21) Krishnaswamy, S. (2005) Exosite-driven substrate specificity and function in coagulation. *J. Thromb. Haemostasis 3*, 54−67.

(22) Newell-Caito, J. L., Griffiths, A. E., and Fay, P. J. (2012) P3-P3′ Residues Flanking Scissile Bonds in Factor VIII Modulate Rates of Substrate Cleavage and Procofactor Activation by Thrombin. *Biochemistry 51*, 3451−3459.

(23) Mimms, L. T., Zampighi, G., Nozaki, Y., Tanford, C., and Reynolds, J. A. (1981) Phospholipid vesicle formation and transmembrane protein incorporation using octyl glucoside. *Biochemistry 20*, 833−840.

(24) Jenkins, P. V., Freas, J., Schmidt, K. M., Zhou, Q., and Fay, P. J. (2002) Mutations associated with hemophilia A in the 558−565 loop

of the factor VIIIa A2 subunit alter the catalytic activity of the factor Xase complex. *Blood 100*, 501−508.
(25) Laemmli, U. K. (1970) Cleavage of structural proteins during the assembly of the head of bacteriophage T4. *Nature 227*, 680−685.
(26) Lollar, P., Fay, P. J., and Fass, D. N. (1993) Factor VIII and factor VIIIa. *Methods Enzymol. 222*, 128−143.
(27) Batty, P., Skelton, S., Shepard, A. J., and Hart, D. P. (2013) Amino acid sequence epitope mapping of four factor VIII monoclonal antibodies. *J. Thromb. Haemostasis 11* (Suppl. 2), 579.
(28) Nogami, K., Wakabayashi, H., and Fay, P. J. (2003) Mechanisms of factor Xa-catalyzed cleavage of the factor VIIIa A1 subunit resulting in cofactor inactivation. *J. Biol. Chem. 278*, 16502−16509.
(29) Bianchini, E. P., Louvain, V. B., Marque, P. E., Juliano, M. A., Juliano, L., and Le Bonniec, B. F. (2002) Mapping of the catalytic groove preferences of factor Xa reveals an inadequate selectivity for its macromolecule substrates. *J. Biol. Chem. 277*, 20527−20534.